Mutations of the Asparagine[117] Residue of a Receptor Activity-Modifying Protein 1-Dependent Human Calcitonin Gene-Related Peptide Receptor Result in Selective Loss of Function†

Remo Gujer,‡ Amaya Aldecoa,‡ Nicole Bühlmann, Kerstin Leuthäuser, Roman Muff, Jan A. Fischer, and Walter Born*

Research Laboratory for Calcium Metabolism, Departments of Orthopedic Surgery and Medicine, University of Zurich, Klinik Balgrist, 8008 Zurich, Switzerland

Received October 30, 2000; Revised Manuscript Received February 15, 2001

ABSTRACT: The initially orphan human calcitonin (CT) receptor-like receptor (hCRLR) interacts with novel accessory receptor activity-modifying protein 1 (RAMP1) to reveal a functional CT gene-related peptide (CGRP) receptor. In mammalian cells, RAMP1 is required for mature N-glycosylation of the hCRLR predicted to occur at Asn[60], Asn[112], and/or Asn[117] in the amino-terminal extracellular domain. Here we have shown that the substitution of Asn[117] with Ala, Gln, Thr, or Pro abolished CGRP-evoked cAMP formation which was left unchanged when the Asn[117] was replaced with Asp. Moreover, the hCRLR and the Asn[117] mutants exhibited comparable N-glycosylation and cell surface expression, and the association with RAMP1 was only slightly impaired. In contrast, the hCRLR Asn[60,112] to Thr double mutant exhibited defective RAMP1-dependent N-glycosylation, and impaired cell surface expression and CGRP receptor function. Unlike Asn[60] and Asn[112], Asn[117] is normally not N-glycosylated, but essential for CGRP binding to the hCRLR−RAMP1 complex.

The α-calcitonin (CT)[1] gene-related peptide (αCGRP) is a 37-amino acid neuropeptide encoded by an alternative mRNA splicing product of the CT gene (*1*). *β*-CGRP is the product of a second gene which differs in humans and rats in three and one amino acid residue from αCGRP, respectively (*2*). CGRP and adrenomedullin (AM) are potent vasodilators. They belong to the CT family of peptides, which includes CT and amylin (*3*). The peptides have in common N-terminal ring structures of six or seven amino acids linked by disulfide bonds between cysteine residues and amidated C-termini, both required for biological activity. α- and *β*-CGRP are widely expressed in the central and peripheral nervous system, and they elicit characteristic biological effects through interaction with G protein-coupled receptors predominantly linked to cAMP production. The initially orphan rat and human (h) CT receptor-like receptors (CRLR) were found to require novel accessory receptor activity-modifying proteins (RAMPs) for expression at the cell surface (*4*−*6*). Moreover, the human and mouse RAMP1, -2, and -3 determined their pharmacology as CGRP or AM receptors (*6*−*8*). The rat CRLR and the human CT receptor isotype 2 (hCTR2) with 60% amino acid sequence homology associate with RAMP1 at the cell surface as two different CGRP receptor subtypes (*9*). hCTR2 coexpressed with RAMP1 or -3 revealed two different amylin receptor isotypes (*10*, *11*).

Here we have investigated RAMP1-associated CGRP receptor function of the hCRLR mutated at the three predicted Asn[60], Asn[112], and Asn[117] N-glycosylation consensus sites that are conserved in all CRLRs identified so far. The results indicate that Asn[60] and/or Asn[112] unlike Asn[117] is required for cell surface expression. With the Asn[117] to Ala, Gln, Thr, and Pro mutants, N-glycosylation and cell surface expression were maintained and the association with RAMP1 was minimally affected, but ligand binding was abolished.

MATERIALS AND METHODS

Materials. Human αCGRP(1−37) was purchased from Bachem. The membrane-impermeable cross-linker bis(sulfosuccinimidyl)suberate (BS3) and ImmunoPure Immobilized Protein G were supplied by Pierce. *N*-Glycosidase F was from Boehringer Mannheim, and restriction enzymes were purchased from Promega. Na[125]I, ECL Western blot detection reagents, and Hybond ECL nitrocellulose membranes were obtained from Amersham Pharmacia Biotech. Tissue culture media and fetal calf serum were obtained from Biological Industries (Kibbutz Beit Haemek). Geneticin 418, LipofectAMINE, or LipofectAMINE 2000 and OptiMEM medium were supplied by Life Technologies. Other chemicals and reagents were purchased from Sigma and Merck at the highest grade available.

Plasmids and Construction of hCRLR Mutants. The cDNA encoding the hCRLR with an N-terminal myc epitope

† This study was supported by the Swiss National Science Foundation, the Kanton of Zurich, and the Schweizerischer Verein Balgrist.

* To whom correspondence should be addressed: Research Laboratory for Calcium Metabolism, Klinik Balgrist, Forchstr. 340, 8008 Zurich, Switzerland. Telephone: +41-1-386-1665. Fax: +41-1-386-1652. E-mail: wborn@balgrist.unizh.ch.

‡ These authors contributed equally to this work.

[1] Abbreviations: CT, calcitonin; AM, adrenomedullin; CGRP, calcitonin gene-related peptide; hCRLR, human calcitonin receptor-like receptor; hCTR2, human calcitonin receptor isotype 2; RAMP, receptor activity-modifying protein.

10.1021/bi002497v CCC: $20.00
Published on Web 04/06/2001

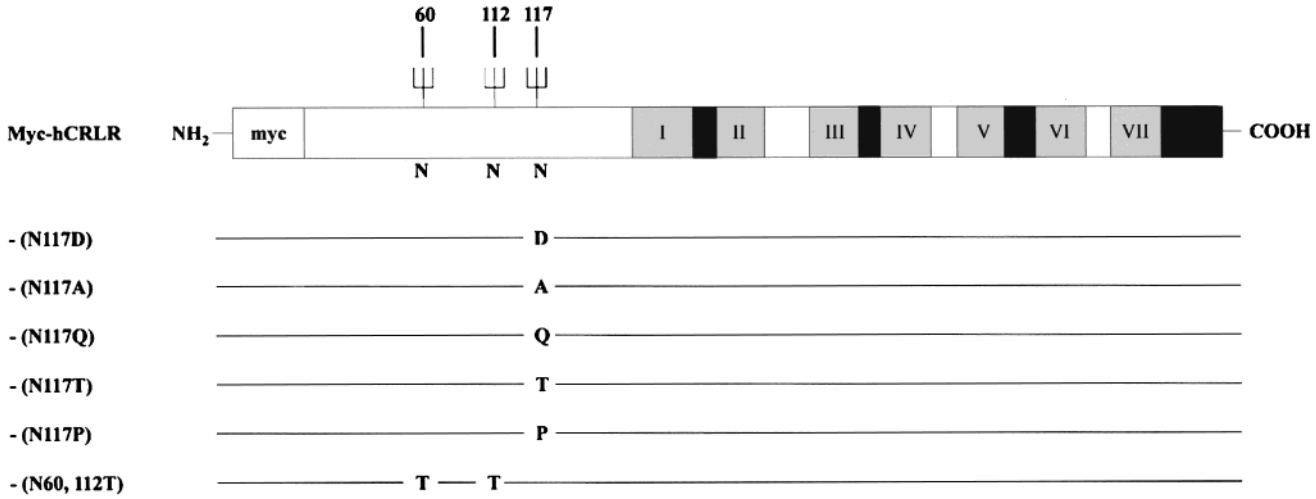

FIGURE 1: Schematic representation of nonmodified and mutant myc-hCRLR. The N-terminal myc epitope, extracellular (white boxes), transmembrane (gray boxes with roman numbers), and intracellular domains (black boxes) are shown. Asparagine (N) residues at positions 60, 112, and 117 are N-glycosylation consensus sites of the myc-hCRLR that were substituted with aspartic acid (D), alanine (A), glutamine (Q), threonine (T), and proline (P) residues as indicated.

(EQKLISEEDLL) (myc-hCRLR) in the mammalian expression vector pcDNA3 (Invitrogen) was provided by S. Foord (GlaxoWellcome). The construct for expression of the hCRLR with C-terminal myc and $(His)_6$ epitope tags (hCRLR-myc) was obtained as follows. A DNA fragment encoding the C-terminus of hCRLR between a unique *Pst*I restriction site and the translational stop codon was amplified by PCR using a 3′-oligonucleotide that introduced a *Hin*dIII recognition sequence in place of the hCRLR translation stop codon. The PCR product was digested with *Hin*dIII, releasing a *Hin*dIII DNA fragment that encoded the C-terminus of hCRLR downstream of a unique *Hin*dIII restriction site in the hCRLR coding sequence with the stop codon removed. This DNA fragment together with a *Bam*HI/*Hin*dIII restriction fragment encoding the remaining N-terminal portion of the hCRLR was cloned into a modified *Bam*HI/*Hin*dIII-digested pcDNA3 expression vector encoding myc and $(His)_6$ downstream of the *Hin*dIII restriction site. This reconstructed the hCRLR coding sequence in frame with the sequence encoding myc and $(His)_6$ at the C-terminus. The cDNA encoding RAMP1 in frame with C-terminal V5-(GKPIPNPLLGLDST) and $(His)_6$ epitope tags was removed by *Kpn*I/*Pme*I digestion from a previously described construct in the *Drosophila* expression vector pAc5.1/V5His (Invitrogen) (*12*) and subcloned into *Kpn*I/*Eco*RV-digested pcDNA3. The three N-glycosylation consensus sequences (Asn-X-Ser/Thr) within the N-terminal extracellular domain of the hCRLR were modified as indicated in Figure 1 through site-directed mutagenesis with the Seamless Cloning Kit (Stratagene). The nucleotide sequence between 5′-*Bsu*36I and 3′-*Pst*I restriction sites encodes the subdomain of the hCRLR that contains all three potential N-glycosylation sites. Pairs of primers were designed to carry out PCR amplification with cloned *Pfu* DNA polymerase (Stratagene) of *Bsu*36I/*Eam*1104I and *Eam*1104I/*Pst*I DNA fragments with the nucleotide substitutions required to create the mutations. The products obtained after 30 cycles were digested with *Eam*1104I and *Bsu*36I or *Pst*I and gel-purified. Ligation of matching fragments into *Bsu*36I/*Pst*I-digested myc-hCRLR reconstituted the coding sequence for the myc-hCRLR-(N60T), -(N112T), -(N117D), -(N117A), -(N117Q), -(N117T), and -(N117P) mutants. The double mutant myc-hCRLR-(N60,112T) was generated by *Bgl*II digestion of *Not*I/*Xho*I DNA fragments of myc-hCRLR(N60T) and of myc-hCRLR-(N112T) and religation of the *Not*I/*Bgl*II fragment containing the N60T mutation and the *Bgl*II/*Xho*I fragment with the N112T mutation into *Not*I/*Xho*I-digested pcDNA3. The nucleotide sequence between the *Bsu*36I and *Pst*I restriction sites in the final hCRLR mutant expression constructs was verified by sequencing in both directions.

Cell Culture and Lipotransfection. COS-7 cells were cultured in a HamF12/DMEM (4.5 g/L glucose) mixture (1:1) supplemented with 10% fetal calf serum and 2 mM glutamine (tissue culture medium). The same medium, supplemented with 400 μg/mL Geneticin 418, was used to culture SV40 T-antigen-transformed human embryonic kidney HEK293 (TSA) cells. The cells were subcultured by treatment with 0.1% trypsin and 0.5 mM EDTA in PBS. Transfections were carried out at 80% confluence by incubating the cells for 4 h at 37 °C in OptiMEM medium containing the indicated concentrations of LipofectAMINE or LipofectAMINE 2000 and plasmid DNA. The experiments were performed 48 h after transfection. The level of cyclic AMP accumulation in transiently transfected COS-7 cells was measured as described previously (*7*).

Cross-Linking, Immunoprecipitation, and Deglycosylation. Transiently transfected TSA cells in 100 mm dishes were incubated with 8×10^4 Bq of [^{125}I]hαCGRP in 4.8 mL of a HamF12/DMEM mixture (1:1) supplemented with 0.1% BSA (binding medium) for 2 h at 15 °C. Subsequently, the cells were washed with PBS and incubated for 1 h at room temperature in 4.8 mL of 0.1 M PBS containing 1 mM cross-linker BS3. Cross-linking was quenched by adding Tris-HCl to a final concentration of 15 mM (pH 7.5). The cells were lysed in 50 mM Hepes (pH 7.5), 7 mM $MgCl_2$, 2 mM EDTA, 1 mM phenylmethanesulfonyl fluoride, 3 μg/mL aprotinin, 3 μg/mL leupeptin, 1 mg/mL dodecyl β-D-maltoside, and 0.2 mg/mL cholesterol hemisuccinate. The cell lysates were cleared by centrifugation for 3 min at 10000*g*. Myc-tagged receptors were immunoprecipitated from cleared lysates at 4 °C by sequential incubation with 50 μL of ImmunoPure Immobilized Protein G for 1 h, 2 μg of myc antibodies for

2 h, and 100 μL of ImmunoPure Immobilized Protein G overnight on an end-over-end rotator. The precipitates were then collected by centrifugation for 5 min at 10000*g*. The pellets were washed three times with 50 mM Hepes (pH 7.5), 7 mM $MgCl_2$, 2 mM EDTA, 1 mM phenylmethanesulfonyl fluoride, 3 μg/mL aprotinin, 3 μg/mL leupeptin, and 0.25 mg/mL dodecyl β-D-maltoside. The immunoextracted proteins were eluted from the pellets by incubation in 80 μL of SDS−PAGE loading buffer for 15 min at 50 °C. The amount of [^{125}I]CGRP in the immunoprecipitates was measured in a γ-counter (Kontron). Deglycosylation of proteins in aliquots of cell lysates was carried out with 4 units of *N*-glycosidase F in 50 μL of 10 mM Tris-HCl (pH 7.5), 10 mM EDTA, 0.1% SDS, 0.5% octyl glucopyranoside, and 1% β-mercaptoethanol for 18 h at 37 °C. The incubations were stopped with SDS−PAGE loading buffer.

Western Blot Analysis. Proteins in cell lysates and immunoextracts were separated by SDS−PAGE and electrotransferred to nitrocellulose Hybond ECL membranes in a Trans-Blot cell (Bio-Rad Laboratories) at 25 V and 4 °C overnight. Immunoblots were blocked with 5% low-fat milk, and the epitope-tagged proteins were visualized by enhanced chemiluminescence with horseradish peroxidase-labeled monoclonal myc and V5 antibodies (1:2000 final dilution) (Invitrogen). Actin as a reference protein for the amount of loaded cell lysates was visualized with monoclonal antibodies to actin (1:3500 final dilution) (Chemicon International) and secondary horseradish peroxidase-conjugated sheep antibodies to mouse immunoglobulins (1:5000 final dilution) (Amersham). Cross-linked [^{125}I]hαCGRP was recognized by autoradiography with Hyperfilm MP film (Amersham).

Immunohistochemistry. TSA cells cultured in tissue culture medium supplemented with 400 μg/mL Geneticin 418 were transiently transfected in 3 mL of OptiMEM medium containing 12 μL of LipofectAMINE 2000 and 2.4 μg of indicated receptor and RAMP1-V5 expression constructs. Forty-eight hours later, the cells were detached with 0.05% EDTA in PBS. Cell surface expression of myc epitope-tagged receptors was estimated by myc immunofluorescence staining of intact cells in suspension. The cells were incubated with mouse monoclonal antibodies to myc (Invitrogen) diluted 1:600 in tissue culture medium for 1 h at room temperature. The same medium was used to wash the cells twice and for the incubation with TRITC-labeled polyclonal rabbit anti-mouse immunoglobulin (1:150 final dilution) (Dako Diagnostics) for 30 min at room temperature. The cells were again washed twice with tissue culture medium and once with PBS. The cells were then fixed with 3% formaldehyde in PBS for 20 min. TRITC fluorescence of equal aliquots of cells was measured in a SpectraMAX GeminiXS fluorescence reader (Molecular Devices) with the excitation at 530 nm, emission at 590 nm, and cutoff at 570 nm. Background fluorescence of the cells transfected with pcDNA3 was subtracted. Fluorescence staining of cells was also visualized by fluorescence microscopy. Aliquots of cells were dried on a slide and mounted with Immu-Mount (Shandon Scientific). The cells were viewed with an Eclipse E600 Nikon microscope with a G2-A filter and 50-fold magnification. Photographs taken from individual slides at a constant exposure time were scanned with an LS-2000 Nikon scanner with the parameters adjusted to minimize background fluorescence.

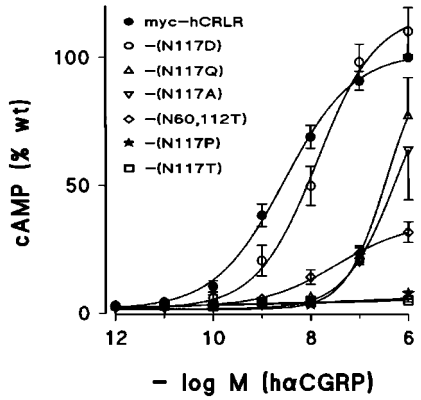

FIGURE 2: Stimulation of cAMP production in COS-7 cells by CGRP. The cells were grown in 24-well plates to 50% confluency. For transfection, the cells were incubated for 4 h at 37 °C in 250 μL of OptiMEM medium containing 200 ng of myc-hCRLR or of the indicated mutants and 200 ng of RAMP1-V5 expression constructs and 1 μL of LipofectAMINE 2000 per well. Forty-eight hours after transfection, the cells were incubated with the indicated concentrations of hαCGRP for 15 min at 37 °C. The results are means ± standard error of the mean of three independent experiments.

Statistical Analysis. The values for half-maximal effective concentrations (EC_{50}) were calculated by nonlinear regression analysis using Fig. P 6.0 software (Biosoft, Cambridge, U.K.), and differences between mean values were analyzed by ANOVA. Differences between mean values of percent cell surface expression of individual myc-hCRLR mutants compared to nonmodified myc-hCRLR controls were analyzed by a Student's *t* test. *P* values of <0.05 were considered statistically significant.

RESULTS

Stimulation of cAMP Production and Cell Surface Expression of Myc-hCRLR and Mutants Thereof Coexpressed with RAMP1-V5. Cyclic AMP accumulation in response to CGRP was estimated in transiently transfected COS-7 cells (Figure 2). In cells expressing the myc-hCRLR and RAMP1-V5, cAMP production was stimulated 36-fold by 10^{-6} M hαCGRP with an EC_{50} of 3.8 ± 1.1 nM ($n = 8$). In cells expressing myc-hCRLR(N60T) or -(N112T) together with RAMP1-V5, the cAMP response was that of the nonmutated myc-hCRLR (not shown), and these mutants were not further investigated. But with the double mutant myc-hCRLR(N60,-112T), cAMP production by 10^{-6} M hαCGRP was lowered to 30% of that of the myc-hCRLR, and the EC_{50} was increased 9-fold. The various amino acid substitutions at Asn^{117} in the myc-hCRLR affected CGRP-evoked stimulation of cAMP formation to a different degree. The cAMP response was similar in cells expressing nonmodified myc-hCRLR or the mutant myc-hCRLR(N117D) both together with RAMP1-V5. But the cAMP production remained at basal levels in cells cotransfected with myc-hCRLR(N117T) or -(N117P) and RAMP1-V5 expression constructs. In the cells expressing myc-hCRLR(N117A) and -(N117Q), hαCGRP stimulated the cAMP production with an EC_{50} of >100 nM.

Myc immunofluorescent staining of intact cells, reflecting receptor cell surface expression, was comparable in TSA cells transiently expressing myc-hCRLR or the N117D, N117A, N117Q, N117T, or N117P mutant together with RAMP1-

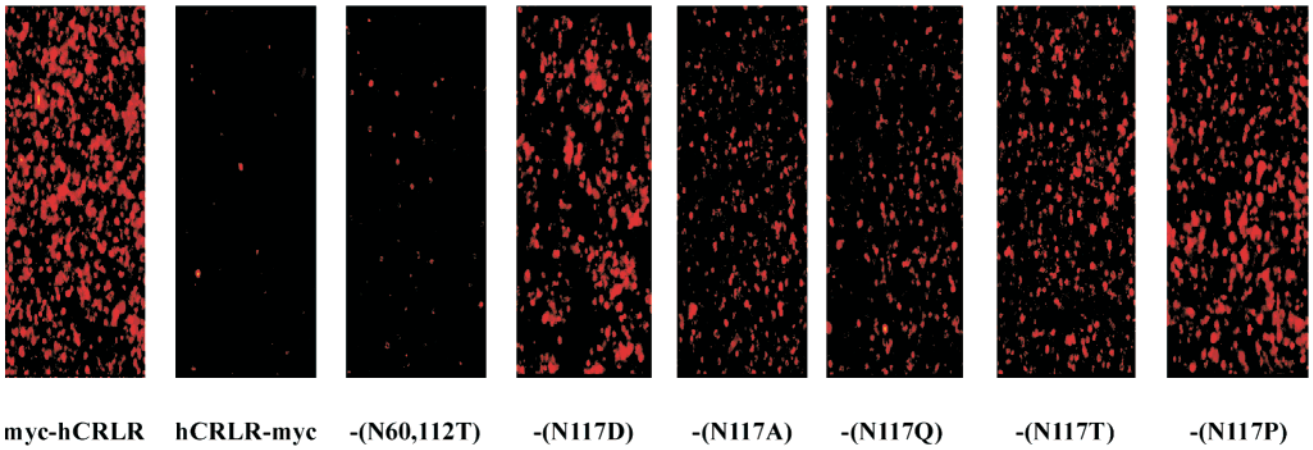

FIGURE 3: Myc immunofluorescent staining of intact TSA cells. The cells were transfected with expression constructs of the RAMP1-V5 and of the hCRLR with myc at the N-terminus (myc-hCRLR) or indicated mutants, or of the hCRLR with myc at the C-terminus (hCRLR-myc) as a negative control. Mouse antibodies to myc and TRITC-labeled rabbit antibodies to mouse immunoglobulins were used to visualize by fluorescence microscopy myc presented at the surface of intact cells. The cells were prepared as described in Materials and Methods.

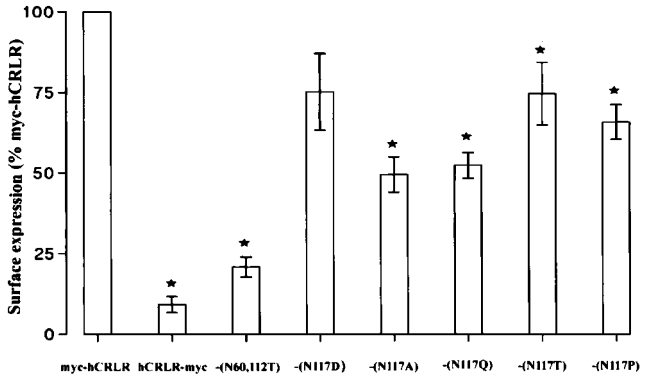

FIGURE 4: Quantitative analysis of myc immunofluorescent staining at the cell surface of intact TSA cells. The cells were transfected and immunostained and prepared for analysis in a fluorescence microplate reader as described in Materials and Methods. Myc immunofluorescence as a measure of receptor cell surface expression was normalized to that of myc-hCRLR. The results are means ± standard error of the mean of four independent experiments. Asterisks denote $P < 0.05$.

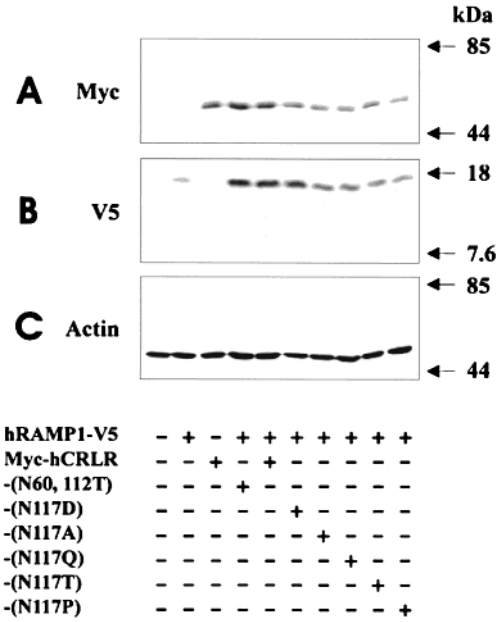

FIGURE 5: Expression levels of myc-hCRLR and its mutants and of coexpressed RAMP1-V5. TSA cells were grown in six-well plates to 80% confluency and transfected by incubation for 4 h at 37 °C in 2 mL of OptiMEM medium containing 4.8 μL of LipofectAMINE and indicated combinations of 67 ng of RAMP1-V5 and 67 ng of myc-hCRLR or mutant expression constructs per well. The expression vector pcDNA3 was used for mock transfections and to equalize the total amount of DNA in individual transfections. Two days later, aliquots of cell extracts were treated with 4 units of *N*-glycosidase F and subjected to 15% SDS−PAGE. Myc-tagged receptors (A) and RAMP1-V5 (B) were visualized on Western blots with HRP-conjugated myc and V5 antibodies. Actin as a reference to control for protein loading was detected with mouse monoclonal antibodies to actin and secondary horseradish peroxidase-conjugated sheep antibodies to mouse immunoglobulins (C). Representative experiment carried out at least three times.

V5, but it was hardly visible in cells expressing myc-hCRLR-(N60,112T) (Figure 3). The hCRLR with a C-terminal, intracellular myc epitope tag, and normal function served as a negative control. Quantitative analysis revealed between 50 and 80% cell surface expression of myc-hCRLR(N117D), -(N117A), -(N117Q), -(N117T), or -(N117P) as compared to the myc-hCRLR, and that of the myc-hCRLR(N60,112T) was less than 25% (Figure 4). Western blot analysis of total cell extracts treated with *N*-glycosidase F showed comparable expression levels of the 58 kDa deglycosylated myc-hCRLR and its mutants in the presence of RAMP1-V5 (Figure 5A).

Taken together, impaired cell surface delivery of myc-hCRLR(N60,112T) as compared to nonmodified myc-hCRLR in the presence of RAMP1-V5 resulted in a reduced CGRP-evoked cAMP response. In contrast, the myc-hCRLR-(N117A), -(N117Q), -(N117T), and -(N117P) lost CGRP receptor function in the face of cell surface expression levels comparable to those of the active myc-hCRLR and its N117D mutant.

Cell Surface Association of RAMP1-V5 with Myc-hCRLR and the Asn[117] Mutants and [^{125}I]hαCGRP Binding in TSA Cells. Mock-transfected cells and cells transiently expressing RAMP1-V5 alone or together with myc-hCRLR or the individual mutants were incubated with [^{125}I]hαCGRP and subsequently treated with the cross-linker BS3. Protein components carrying myc epitope tags were immunoprecipitated from cell homogenates with the corresponding antibodies. The amount of coprecipitated [^{125}I]hαCGRP was estimated in a γ-counter, and [^{125}I]hαCGRP−binding protein components were characterized by autoradiography and on

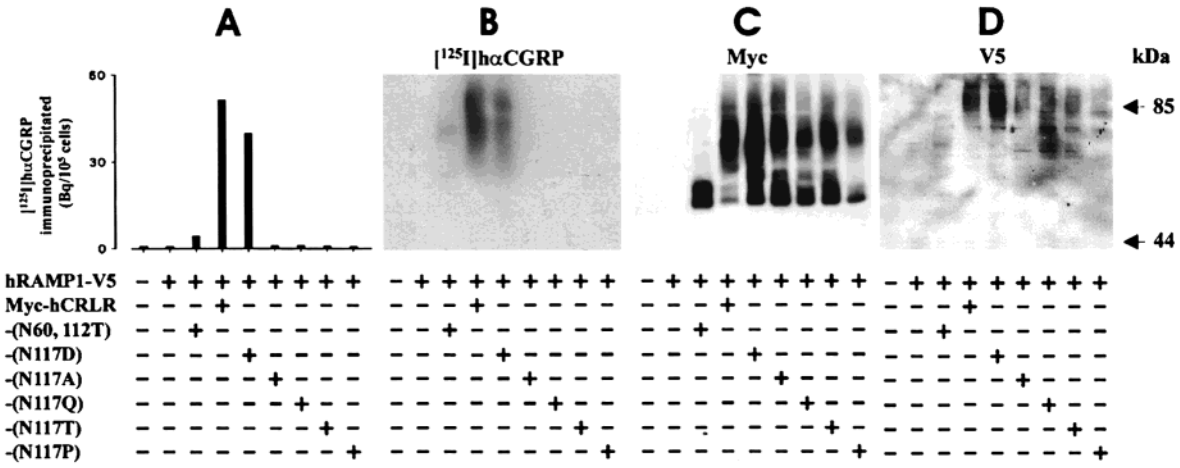

FIGURE 6: Immunoextraction with myc antibodies of [^{125}I]hαCGRP cross-linked to wild-type and mutant myc-hCRLR−RAMP1-V5 complexes (A) and analysis on Western blots by autoradiography (B) and with myc (C) and V5 antibodies (D). TSA cells were grown in 100 mm dishes to 80% confluency. They were then transfected in 12 mL of OptiMEM medium containing 29 μL of LipofectAMINE and 800 ng of pcDNA3 (mock transfection) or 400 ng of RAMP1-V5 expression construct together with 400 ng of pcDNA3 or together with 400 ng of myc-hCRLR or the indicated mutant myc-hCRLR expression constructs per dish. Two days after transfection [^{125}I]hαCGRP binding, protein cell surface cross-linking, immunoextractions and autoradiography, and Western blot analysis of immunoextracted proteins subjected to 10% SDS−PAGE were carried out as described in Materials and Methods. Representative experiment carried out three times.

Western blots with antibodies to the myc-hCRLR and the RAMP1-V5 (Figure 6). Autoradiography revealed [^{125}I]hαCGRP-labeled proteins of 68 and 83 kDa in TSA cells expressing myc-hCRLR or -(N117D) together with RAMP1-V5 (Figure 6B). In immunoprecipitates obtained from mock-transfected cells or from cells expressing RAMP1-V5 alone or with myc-hCRLR(N117A), -(N117Q), -(N117T), or -(N117P), [^{125}I]hαCGRP-labeled proteins were undetectable. In cells expressing myc-hCRLR(N60,112T) with RAMP1-V5, a 68 kDa [^{125}I]hαCGRP-labeled protein was observed. A 62 kDa protein was barely detectable.

On the same Western blots, myc immunoreactive protein components were undetectable in extracts of mock-transfected cells or cells expressing RAMP1-V5 alone. A myc immunoreactive protein doublet of 58 and 60 kDa was observed in extracts of cells expressing myc-hCRLR(N60,-112T) and RAMP1-V5 (Figure 6C). The size of the lower-molecular mass band corresponds to the 58 kDa myc-hCRLR deglycosylated with *N*-glycosidase F (Figure 5A), indicating impaired N-glycosylation of myc-hCRLR(N60,112T). The larger 60 kDa band is resistant to *N*-glycosidase F treatment (not shown) and likely indicates another secondary myc-hCRLR modification. Protein doublets of the same size were also recognized in extracts of cells expressing RAMP1-V5 together with myc-hCRLR and the various Asn^{117} mutants. But all these samples contained additional myc-tagged proteins with the size of the 68 and 83 kDa [^{125}I]hαCGRP-labeled components detected in extracts of cells expressing myc-hCRLR that is known to undergo mature N-glycosylation in the presence of RAMP1 (*6*). The size difference of the 68 and 83 kDa protein components corresponded to the molecular mass calculated for RAMP1-V5.

The same Western blots were subsequently analyzed with V5 antibodies (Figure 6D). In myc immunoextracts of cells expressing myc-hCRLR(N60,112T) together with RAMP1-V5, a V5-tagged 70 kDa protein was observed. This protein component was undetectable in mock- or RAMP1-V5-transfected cells, and its size was consistent with nonglycosylated myc-hCRLR(N60,112T) cross-linked with RAMP1-V5. In cells expressing nonmodified myc-hCRLR or the myc-hCRLR Asn^{117} mutants together with RAMP1-V5, V5 immunoreactive protein components extracted with myc antibodies were 83 kDa in size, equal to the largest proteins recognized with myc antibodies and by autoradiography. Discrete bands of approximately 90 kDa detected with V5 antibodies were hardly visible with myc antibodies and on autoradiography, and their molecular composition remains to be identified. Extracts of cells expressing RAMP1-V5 together with myc-hCRLR(N117A), -(N117Q), or -(N117T) contained additional V5-tagged proteins similar to the 70 kDa V5 immunoreactive component in extracts of myc-hCRLR(N60,112T) and RAMP1-V5 coexpressing cells. The size is consistent with nonglycosylated mutant myc-hCRLR−RAMP1 complexes, indicating that mature N-glycosylation of these mutants occurs less efficiently than that of myc-hCRLR.

Taken together, the results indicate co-immunoprecipitation of RAMP1-V5 cross-linked to mutant and nonmodified myc-hCRLR at the cell surface. But, [^{125}I]hαCGRP binding occurred only in cells expressing myc-hCRLR or -(N117D) together with RAMP1-V5, and the level of binding was lower in cells exhibiting impaired cell surface expression and N-glycosylation of myc-hCRLR(N60,112T) also in the presence of RAMP1-V5 (Figures 3 and 4). The difference in size between the 68 and 83 kDa radiolabeled protein components in cells coexpressing myc-hCRLR or -(N117D) and RAMP1-V5 and the fact that the 68 kDa components were recognized by the myc but not by the V5 antibodies indicated cross-linking of [^{125}I]hαhCGRP to the 68 kDa receptors alone and to 83 kDa receptor−RAMP1-V5 complexes visualized by myc and V5 antibodies. A [^{125}I]hαCGRP−RAMP1-V5 cross-linking product in immunoextracts obtained with V5 antibodies was not detectable (not shown). But, inefficient cross-linking due to a limited number of reactive NH_2 groups available in [^{125}I]hαCGRP and RAMP1-V5 has to be considered, and the possibility of a direct interaction of RAMP1 and hαCGRP upon its binding to the hCRLR−RAMP1 complex cannot be excluded.

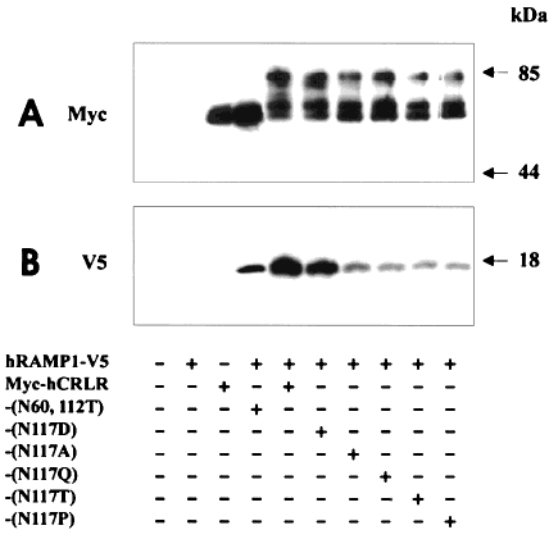

FIGURE 7: Co-immunoprecipitation of RAMP1-V5 with myc-hCRLR and the indicated mutants. TSA cells were grown and transfected as described in the legend of Figure 6. Proteins immunoprecipitated with myc antibodies from cell lysates were subjected to 15% SDS−PAGE, and Western blots were analyzed with HRP-conjugated myc (A) and V5 antibodies (B). Representative experiment carried out three times.

Co-Immunoprecipitation of hRAMP1-V5 with Myc-hCRLR and Its Asn[117] Mutants in the Absence of Cross-Linker. Myc epitope-carrying protein components were immunoextracted from TSA cell homogenates and characterized on Western blots with myc and V5 antibodies (Figure 7). In extracts of mock-transfected cells or of cells expressing RAMP1-V5 alone, myc and V5 immunoreactive proteins remained undetectable. Immunoextracts of cells expressing myc-hCRLR alone or of cells coexpressing myc-hCRLR(N60,-112T) and RAMP1-V5 contained myc-hCRLR with an apparent M_r of 58 000 (Figure 7A). In TSA cells coexpressing myc-hCRLR or its different Asn[117] mutants and RAMP1-V5, major protein components were 68 kDa in size. This indicated RAMP1-dependent N-glycosylation of the hCRLR in mammalian cells that was reversed when the cell extracts were treated with *N*-glycosidase F (Figure 5A). RAMP1-V5 co-immunoprecipitated with wild-type and all mutant myc-hCRLR, and was recognized with V5 antibodies at its predicted size of 14 kDa (Figure 7B). In the face of comparable amounts of myc-hCRLR and individual mutants recognized on Western blots, the amounts of coprecipitated RAMP1-V5 varied between the different extracts. They were higher in extracts of cells expressing the functional myc-hCRLR and -(N117D) CGRP receptors. In total cell homogenates, on the other hand, the RAMP1-V5 expression levels paralleled those of deglycosylated myc-hCRLR and its mutants (Figure 5A,B). In extracts of cells expressing RAMP1-V5 alone, the amounts were smaller than in cells coexpressing myc-hCRLR or its mutants.

Taken together, the results indicate association of RAMP1-V5 with nonmodified myc-hCRLR and all the mutants. In cells expressing the functionally defective myc-hCRLR mutants, the fractions of RAMP1-V5 associated with the receptors in immunoprecipitable complexes were smaller than in extracts of cells expressing the functional myc-hCRLR or its N117D mutant. Misfolding of the inactive receptor−RAMP1 complexes associated with reduced stability has to be considered.

DISCUSSION

The recognition sequence for N-linked glycosylation is Asn-X-Ser/Thr. Substitution of Asn with a different amino acid eliminates N-glycosylation at a particular consensus site. Mutations of the Asn residues are therefore used to dissect the functional importance of individual N-glycosylation sites.

Here, the three predicted N-glycosylation sites, Asn[60], Asn[112], and Asn[117], of the hCRLR have been mutated, and CGRP receptor function has been analyzed in the presence of RAMP1. Our study focused on CGRP-evoked cAMP production, surface expression, and the association with RAMP1 in cells expressing individual Asn mutants together with RAMP1. The Asn[60] and Asn[112] to Thr mutants exhibited normal CGRP receptor function and were not further investigated. Adenylyl cyclase activation by CGRP, on the other hand, was impaired by Asn[117] to Ala or Gln substitutions and abolished when Asn[117] was replaced with Thr or Pro. Importantly, Asp in the place of Asn[117] did not affect CGRP receptor activity of the myc-hCRLR. All Asn[117] hCRLR mutants maintained more than 50% cell surface expression approaching the nonmodified myc-hCRLR. The fraction of RAMP1-V5 that co-immunoprecipitated with the defective myc-hCRLR Asn[117] mutants was lower than that in cells expressing the functionally active myc-hCRLR or its myc-hCRLR(N117D) mutant. The findings point to an impaired formation or stability of the inactive mutant receptor−RAMP1 complexes.

Mature N-glycosylation of the myc-hCRLR and of all the Asn[117] mutants occurred to the same apparent size of 68 kDa, but the proportion of the 58 kDa non-N-glycosylated receptor was larger for the mutants than for the unaltered myc-hCRLR. This and the fact that the Asn[117] to Asp mutant of the myc-hCRLR has no functional defect indicate that Asn[117] is not normally used for N-glycosylation. But its substitution may reduce the efficiency of N-glycosylation at Asn[60] and Asn[112]. Asn[117] may not be accessible for N-glycosylation in the nonmutated myc-hCRLR−RAMP1 complex. If it is assumed that a stable and properly folded hCRLR−RAMP1 complex is a prerequisite for N-glycosylation of the receptor, the impaired mutant myc-hCRLR−RAMP1 complex formation or stability observed for the Asn[117] to Ala, Gln, Thr, and Pro mutants may account for their less efficient mature N-glycosylation.

Since the Asn[117] to Asp substitution does not affect myc-hCRLR function, the introduction of a negative charge in an otherwise unaltered side chain of the amino acid residue in position 117 does not disturb the active conformation, and the hCRLR−RAMP1 association was not affected. The amino acid sequence flanking Asn[117] of the hCRLR is highly conserved among CRLR, CTR, and parathyroid hormone receptors of different species all belonging to the B family of G protein-coupled receptors. Analysis of the N-terminal extracellular domain of the myc-hCRLR with the GOR IV secondary structure prediction method (*13*) revealed limited five- to seven-amino acid β-sheet and extensive random coil structure flanking Asn[117] with no obvious alterations by the Asn[117] substitutions. Thus, interpretation of these findings awaits more detailed functional analysis of alterations by

mutations in the amino acid sequences adjacent and distant from Asn^{117}. An analysis of the AM receptor function of all the myc-hCRLR Asn^{117} mutants in the presence of RAMP2 should be included.

The $Asn^{60/112}$ to Thr double mutant of the myc-hCRLR revealed functional defects different from those of the Asn^{117} mutants. Here, N-glycosylation and therefore cell surface expression were impaired. But, the myc-hCRLR(N60,112T) that reached the cell surface revealed specific [^{125}I]hαCGRP binding and adenylyl cyclase activation by CGRP with an EC_{50} similar to that of the nonmodified myc-hCRLR. Limited N-glycosylation at Asn^{117} when Asn^{60} and Asn^{112} are both mutated may explain the reduced level of cell surface expression of the myc-hCRLR(N60,112T).

Like the inactive myc-hCRLR Asn^{117} mutants, the fraction of RAMP1 associated with myc-hCRLR(N60,112T), as revealed by co-immunoprecipitation, was diminished compared to that of the functional myc-hCRLR and myc-hCRLR-(N117D). Together, the results indicate that N-glycosylation of the hCRLR is required for transport to the cell surface. But defective N-glycosylation through mutations of both Asn^{60} and Asn^{112} does not preclude close to normal interaction of hCRLR with CGRP and RAMP1.

In conclusion, the substitution of Asn residues in the three N-glycosylation consensus sequences of the hCRLR causes two distinct functional deficits. The hCRLR $Asn^{60,112}$ to Thr mutant exhibits defective N-glycosylation and impaired cell surface delivery. The Asn^{117} to Ala, Gln, Thr, and Pro mutations, on the other hand, did not impair cell surface expression to any great extent, but abolished the functional interaction with CGRP. The hCRLR−RAMP1 association required for CGRP receptor function was only slighty impaired by the amino acid substitutions, but misfolding and decreased stability of the mutant receptor−RAMP1 complexes presumably contribute to the functional defect.

REFERENCES

1. Amara, S. G., Jonas, V., Rosenfeld, M. G., Ong, E. S., and Evans, R. M. (1982) *Nature 298*, 240−244.
2. Steenbergh, P. H., Höppener, J. W. M., Zandberg, J., Lips, G. J. M., and Jansz, H. S. (1985) *FEBS Lett. 2488*, 403−407.
3. Wimalawansa, S. J. (1996) *Endocr. Rev. 17*, 533−585.
4. Chang, C. P., Pearse, R. V., II, O'Connell, S., and Rosenfeld, M. G. (1993) *Neuron 11*, 1187−1195.
5. Flühmann, B., Muff, R., Hunziker, W., Fischer, J. A., and Born, W. (1995) *Biochem. Biophys. Res. Commun. 206*, 341−347.
6. McLatchie, L. M., Fraser, N. L., Main, M. J., Wise, A., Brown, J., Thomson, N., Solari, R., Lee, M. G., and Foord, S. M. (1998) *Nature 393*, 333−339.
7. Bühlmann, N., Leuthäuser, K., Muff, R., Fischer, J. A., and Born, W. (1999) *Endocrinology 140*, 2883−2890.
8. Husmann, K., Sexton, P. M., Fischer, J. A., and Born, W. (2000) *Mol. Cell. Endocrinol. 162*, 35−43.
9. Leuthäuser, K., Gujer, R., Aldecoa, A., McKinney, R. A., Muff, R., Fischer, J. A., and Born, W. (2000) *Biochem. J. 351*, 347−351.
10. Muff, R., Bühlmann, N., Fischer, J. A., and Born, W. (1999) *Endocrinology 140*, 2924−2927.
11. Christopoulos, G., Perry, K. J., Morfis, M., Tilakaratne, N., Gao, Y., Fraser, N. J., Main, M. J., Foord, S. M., and Sexton, P. M. (1999) *Mol. Pharmacol. 56*, 235−242.
12. Aldecoa, A., Gujer, R., Fischer, J. A., and Born, W. (2000) *FEBS Lett. 471*, 156−160.
13. Garnier, J., Gibrat, J. F., and Robson, B. (1996) *Methods Enzymol. 266*, 540−553.

BI002497V